





## Article

# Combined Therapy of A<sub>1</sub>AR Agonists and A<sub>2A</sub>AR Antagonists in Neuroinflammation

Gabriella Marucci, Diego Dal Ben , Catia Lambertucci , Aleix Martí Navia , Andrea Spinaci, Rosaria Volpini  and Michela Buccioni \*

Medicinal Chemistry Unit, School of Pharmacy, University of Camerino, 62032 Camerino, MC, Italy; gabriella.marucci@unicam.it (G.M.); diego.dalben@unicam.it (D.D.B.); catia.lambertucci@unicam.it (C.L.); aleix.martinavia@unicam.it (A.M.N.); andrea.spinaci@unicam.it (A.S.); rosaria.volpini@unicam.it (R.V.)

\* Correspondence: michela.buccioni@unicam.it; Tel.: +39-0737-402205

**Abstract:** Alzheimer's, Parkinson's, and multiple sclerosis are neurodegenerative diseases related by neuronal degeneration and death in specific areas of the central nervous system. These pathologies are associated with neuroinflammation, which is involved in disease progression, and halting this process represents a potential therapeutic strategy. Evidence suggests that microglia function is regulated by A<sub>1</sub> and A<sub>2A</sub> adenosine receptors (AR), which are considered as neuroprotective and neurodegenerative receptors, respectively. The manuscript's aim is to elucidate the role of these receptors in neuroinflammation modulation through potent and selective A<sub>1</sub>AR agonists (N<sup>6</sup>-cyclopentyl-2'- or 3'-deoxyadenosine substituted or unsubstituted in 2 position) and A<sub>2A</sub>AR antagonists (9-ethyl-adenine substituted in 8 and/or in 2 position), synthesized in house, using N13 microglial cells. In addition, the combined therapy of A<sub>1</sub>AR agonists and A<sub>2A</sub>AR antagonists to modulate neuroinflammation was evaluated. Results showed that A<sub>1</sub>AR agonists were able, to varying degrees, to prevent the inflammatory effect induced by cytokine cocktail (tumor necrosis factor (TNF)-α, interleukin (IL)-1β, and interferon (IFN)-γ), while A<sub>2A</sub>AR antagonists showed a good ability to counteract neuroinflammation. Moreover, the effect achieved by combining the two most effective compounds (**1** and **6**) in doses previously found to be non-effective was greater than the treatment effect of each of the two compounds used separately at maximal dose.

**Keywords:** A<sub>1</sub>AR agonist; A<sub>2A</sub>AR antagonist; combination therapy; neuroinflammation; cytokine; neuroprotection



**Citation:** Marucci, G.; Ben, D.D.; Lambertucci, C.; Navia, A.M.; Spinaci, A.; Volpini, R.; Buccioni, M. Combined Therapy of A<sub>1</sub>AR Agonists and A<sub>2A</sub>AR Antagonists in Neuroinflammation. *Molecules* **2021**, *26*, 1188. <https://doi.org/10.3390/molecules26041188>

Academic Editors: Athina Geronikaki and Jose Luis Lavandera

Received: 10 December 2020

Accepted: 18 February 2021

Published: 23 February 2021

**Publisher's Note:** MDPI stays neutral with regard to jurisdictional claims in published maps and institutional affiliations.



**Copyright:** © 2021 by the authors. Licensee MDPI, Basel, Switzerland. This article is an open access article distributed under the terms and conditions of the Creative Commons Attribution (CC BY) license (<https://creativecommons.org/licenses/by/4.0/>).

## 1. Introduction

In recent years, many research efforts have been directed to neuroinflammation and neuroimmunology, since neurodegenerative diseases such as Alzheimer's disease (AD), Parkinson's disease (PD), and multiple sclerosis (MS) are commonly associated with neuroinflammation induced by activation of microglial cells. In the brain, microglial cells comprise only 5–10% of the total cell population but play a crucial role in dynamic remodeling of the central nervous system (CNS) [1–4]. These cells are activated in response to changes in brain homeostasis, acquiring phagocytic properties and the ability to release a number of pro-inflammatory molecules [5]. This situation produces a neuroinflammatory reaction, which leads to aggravate neurodegenerative diseases. In addition, chronic neuroinflammation is also implicated in pathology progression; therefore, blockade of this reaction may be expected to improve the outcome of neurodegenerative diseases. Microglia activation involves many signaling pathways, cytokines, and growth factors. Hence, the discovery of drugs that selectively suppress the deleterious effects of microglial activation without compromising its beneficial functions is of primary importance. In recent years, endogenous nucleotides and adenosine (Ado) have been shown to be key messengers in microglial activation process [6,7]. In particular, Ado has been widely recognized as an inhibitory modulator of the CNS [8]. It participates in many functions such as homeostatic

modulator at the synapse level, modulating the neuronal excitability, synaptic plasticity, and release of neurotransmitters and is involved in local inflammatory processes [8–13]. In addition, during the inflammatory process, extracellular Ado, a ubiquitous molecule implicated in neuromodulation, reaches high concentrations capable of activating the Ado receptors (ARs)  $A_1$ -,  $A_{2A}$ -,  $A_{2B}$ -, and  $A_3$ AR [11].

In particular,  $A_1$ AR and  $A_{2A}$ AR are primarily involved in neuroinflammation modulation [14]. The  $A_1$ AR is expressed in microglia and plays an important role in microglia activation [15]. Activation of  $A_1$ AR produces both pro-inflammatory and anti-inflammatory responses due to different Ado concentrations [16]. In fact, the activation of  $A_1$ AR by low concentrations of adenosine induces neutrophil chemotaxis and adherence to the endothelium [17]; on the contrary, high concentrations of adenosine induce anti-adhesive effects [18]. A study performed with full agonists, as well as the referent compound CCPA (2-chloro- $N^6$ -cyclopentyladenosine), showed a good effect to activate this receptor, but the full agonist for human therapies is correlated to agonist-induced desensitization on the receptor [19] and a variety of side effects. For this reason, in this study, partial agonists synthesized in house were used, which are derivatives of the reference compound. The partial agonist behavior could be beneficial in the treatment of acute and chronic diseases due to less side effects with respect to the reference compound  $A_1$ AR full agonist [20].

In brain injury models, inflammation induced by  $A_{2A}$ AR activation, as well as secretion of interleukin (IL)-18 mediators such as IL-12, interferon (IFN)- $\gamma$ , and tumor necrosis factor (TNF)- $\alpha$ , was abolished by  $A_1$ AR activation [21], producing a neuroprotective effect in pathological conditions [22]. Moreover, the  $A_{2A}$ AR is the most implicated adenosine receptor in neuroinflammation [23]. It is worth noting that  $A_{2A}$ AR expression in microglia is usually low, but it increases as a result of brain insults. In microglial cells, when  $A_{2A}$ AR overexpression was activated, cytokine release [24] and change in amoeboid morphology occurred [25]. On the contrary,  $A_{2A}$ AR antagonists suppress microglia activation [26]. Despite the reference compound ZM241385 (4-(2-[7-Amino-2-(2-furyl)[1,2,4]triazolo[2,3-a][1,3,5]triazin-5-ylamino]ethyl)phenol) being the most active  $A_{2A}$ AR antagonist and, therefore, a useful tool for characterization of responses mediated by  $A_{2A}$ AR, it also acts as an  $A_{2B}$ AR antagonist and blocks the cardioprotective effect of adenosine [27]. Hence, in this study,  $A_{2A}$ AR antagonists synthesized in house with a high selectivity vs.  $A_{2B}$ AR were used.

## 2. Results

The involvement of  $A_1$ AR and  $A_{2A}$ AR in neuroinflammation was investigated in the microglial cell line N13 since it is a very interesting model, as the cells behave in the CNS parenchyma as macrophages and are involved in many different neurodegenerative disease processes and traumatic brain and spinal cord injuries.

The presence of  $A_1$ AR and  $A_{2A}$ AR was identified by direct immunocytochemistry using specific polyclonal antibodies (pAbs). The results showed that the amount of receptors was enough to proceed with biological studies to elucidate the relationship between these two receptors and the neuroinflammation process. Experiments were carried out using Alexa Fluor conjugated pAbs and results are shown in Figure 1.

These results obtained in N13 cells, supported by Borea's and Luongo's investigations [15,28], allowed to study ligand effects in cell viability. The study was carried out using the CellTiter 96<sup>®</sup> AQueous One Solution Cell Proliferation Assay. According to the  $K_i$  value obtained in binding assays, three different concentrations (Table 1) for each compound were tested at 15 and 30 min of incubation. CCPA and ZM241385 were chosen as the reference compounds for the  $A_1$ - and  $A_{2A}$ ARs, respectively. Each ligand (1–6) was tested at three different concentrations according to the  $K_i$  values obtained in the binding assays. The concentrations used were around their  $K_i$  value at 15 and 30 min incubation time (Tables 1 and 2).

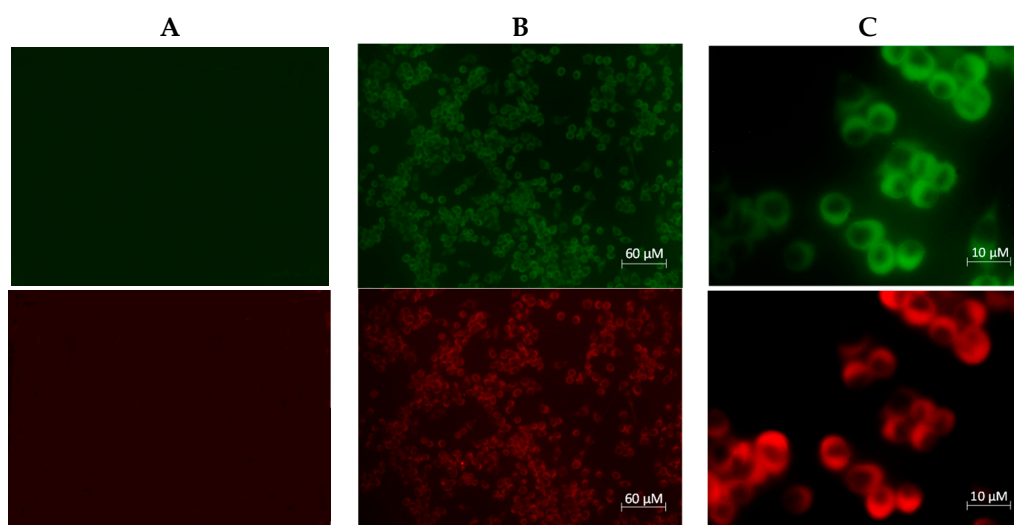
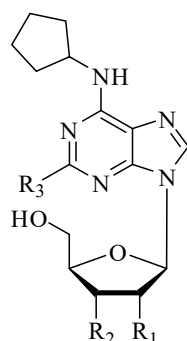


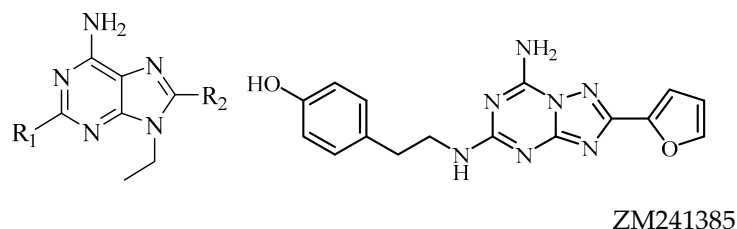
**Figure 1.** Double immunofluorescence staining of N13 cell cultures. Cells were treated with A<sub>1</sub> adenosine receptor (AR) polyclonal antibody Alexa Fluor<sup>®</sup> 488-conjugated (green) and adenosine A<sub>2A</sub> receptor antibody Alexa Fluor<sup>®</sup> 594-conjugated (red). (A) Negative staining performed in Chinese Hamster Ovary (CHO) wild-type (WT) cells not expressing the adenosine receptors; (B) staining of A<sub>1</sub>- and A<sub>2A</sub> AR with Alexa Fluor antibodies (10× magnification); (C) staining of A<sub>1</sub>- and A<sub>2A</sub> AR with Alexa Fluor antibodies (60× magnification).

**Table 1.** Biological activity of A<sub>1</sub>AR compounds studied and reference ligand at human (h)ARs<sup>a</sup> [19,20].



Compound	R <sub>1</sub>	R <sub>2</sub>	R <sub>3</sub>	<sup>b</sup> hA <sub>1</sub> K <sub>i</sub> nM	<sup>c</sup> hA <sub>2A</sub> K <sub>i</sub> nM	<sup>e</sup> hA <sub>2B</sub> EC <sub>50</sub> nM	<sup>d</sup> hA <sub>3</sub> K <sub>i</sub> nM
1	H	OH	H	816	>30,000	>30,000	>30,000
2	OH	H	H	10.5 (±1.8)	16,000 (±714)	>30,000	7190 (±510)
3	OH	H	Cl	10.4 (±2)	10,400 (±806)	>30,000	5300 (±1081)
CCPA	OH	OH	Cl	1.2 (±0.2)	2050 (±400)	18,800 (±320)	26 (±5)

<sup>a</sup> Data ( $n = 3-5$ ) are expressed as means  $\pm$  standard errors. <sup>b</sup> Displacement of specific [<sup>3</sup>H]-CCPA binding at hA<sub>1</sub>AR expressed in CHO cells. <sup>c</sup> Displacement of specific [<sup>3</sup>H]-NECA binding at hA<sub>2A</sub>AR expressed in CHO cells. <sup>d</sup> Displacement of specific [<sup>3</sup>H]-HEMADO binding at hA<sub>3</sub>AR expressed in CHO cells. <sup>e</sup> EC<sub>50</sub> value (nM) of adenylyl cyclase activity stimulation in CHO cells expressing hA<sub>2B</sub>AR.

**Table 2.** Biological activity of A<sub>2A</sub>AR compounds studied and reference ligand at human (h)ARs <sup>a</sup> [19,20].

Compound	R <sub>1</sub>	R <sub>2</sub>	hA <sub>1</sub> <sup>b</sup> K <sub>i</sub> nM	hA <sub>2A</sub> <sup>c</sup> K <sub>i</sub> nM	hA <sub>2B</sub> <sup>e</sup> IC <sub>50</sub> * K <sub>i</sub> nM	hA <sub>3</sub> <sup>d</sup> K <sub>i</sub> nM
4	H	OCH <sub>2</sub> CH <sub>3</sub>	752 (±188)	45 (±13)	7940 (±1588)	>30,000
5	H	2-Furyl	49 (±9)	2.6 (±0.4)	1000 (±100)	4700 (±890)
6	OCH <sub>2</sub> CH <sub>3</sub>	OCH <sub>2</sub> CH <sub>3</sub>	4247 (±842)	32 (±6.3)	4860 (±516)	948 (±187)
ZM241385	—	—	255 (±35)	1 (±0.18)	* 50 (±0.11)	>30,000

<sup>a</sup> Data ( $n = 3-5$ ) are expressed as means  $\pm$  standard errors. <sup>b</sup> Displacement of specific [<sup>3</sup>H]-CCPA binding at hA<sub>1</sub>AR expressed in CHO cells. <sup>c</sup> Displacement of specific [<sup>3</sup>H]-NECA binding at hA<sub>2A</sub>AR expressed in CHO cells. <sup>d</sup> Displacement of specific [<sup>3</sup>H]-HEMADO binding at hA<sub>3</sub>AR expressed in CHO cells. <sup>e</sup> IC<sub>50</sub> values of NECA-stimulated adenylyl cyclase activity inhibition in CHO cells expressing hA<sub>2B</sub>AR. \* Ongini et al. 1999 [29].

Since these compounds are known, the binding results are already published [30,31].

The concentrations used for A<sub>1</sub>AR agonists were as follows: compound 1—4, 8, and 50  $\mu$ M; compounds 2 and 3—0.05, 0.1, and 0.6  $\mu$ M, in comparison with CCPA at 0.005, 0.01, and 0.06  $\mu$ M (Table 3). In addition, the concentrations studied for A<sub>2A</sub>AR antagonists were as follows: compound 4—0.2, 0.45, and 2.7  $\mu$ M; compound 5—0.02, 0.04, and 0.25  $\mu$ M; compound 6—0.15, 0.3, and 2  $\mu$ M, in comparison with ZM241385 at 0.005, 0.01, and 0.06  $\mu$ M (Table 3).

**Table 3.** A. Concentrations of A<sub>1</sub>AR ligands tested.

Compound	Concentration 1 ( $\mu$ M)	Concentration 2 ( $\mu$ M)	Concentration 3 ( $\mu$ M)
CCPA	0.005	0.01	0.06
1	4	8	50
2	0.05	0.1	0.6
3	0.05	0.1	0.6
B. Concentrations of A <sub>2A</sub> AR ligands tested			
ZM241385	0.005	0.01	0.06
4	0.2	0.45	2.7
5	0.02	0.04	0.25
6	0.15	0.3	2

The concentrations of the reference compounds were the same, since CCPA for A<sub>1</sub>AR and ZM241385 for A<sub>2A</sub>AR showed identical K<sub>i</sub> values (1.2 nM).

The results showed that cell viability was increased with respect to the control for both CCPA and ZM241385 at all concentrations. The highest effect for both was observed at 0.005  $\mu$ M (139%  $\pm$  4.6 and 119%  $\pm$  3.4 vs. control, respectively) after 30 min of incubation (Figures 2 and 3).

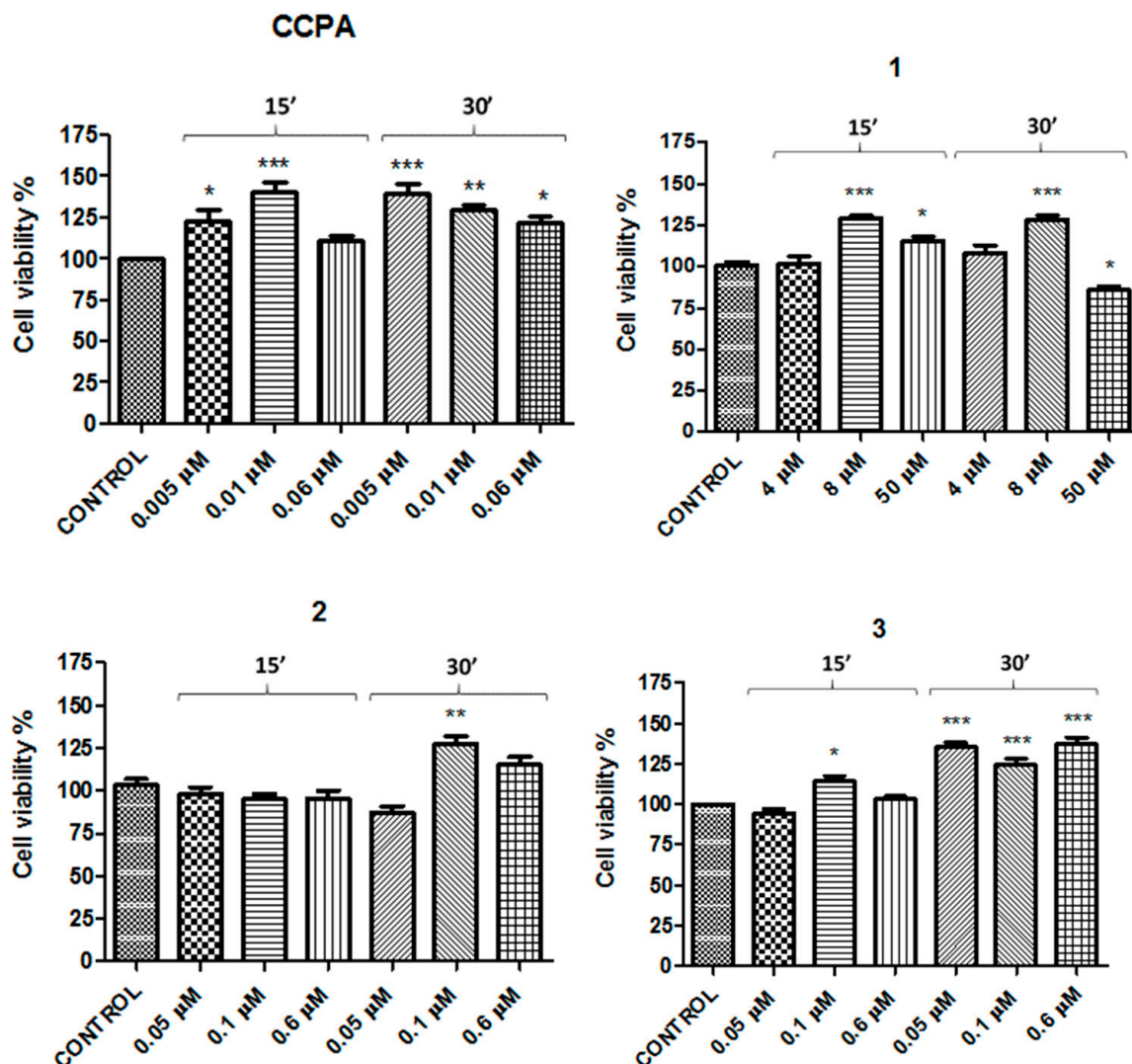


**Figure 2.** Effects of CCPA and compounds 1–3 on N13 cells. Percentage of cell viability after treatment with different ligand concentrations for 15 or 30 min of incubation. Results represent the average of 3–5 independent experiments. \*  $p < 0.05$ , \*\*  $p < 0.01$ , \*\*\*  $p < 0.001$  (one-way ANOVA followed by Dunnett's multiple comparison test of treated cells against control).

Compounds 1, 2, and 3 also exhibited good viability results at all concentrations used, with the exception of compounds 1 and 2 at the highest and the lowest concentrations of 50 and 0.05  $\mu\text{M}$  after 30 min of incubation, respectively, in which there was a decrease in cell viability with respect to the control (Figure 2).

The  $A_{2A}AR$  antagonists (4–6) also appeared to increase the cell viability with respect to the control at all concentrations tested. It is important to note that compounds 4 and 6 increased cell viability in a significant manner, in particular at 0.45 and 0.3  $\mu\text{M}$  at 30 min, respectively ( $133\% \pm 5.5$  and  $129\% \pm 3.5$  vs. control, respectively) (Figure 3).



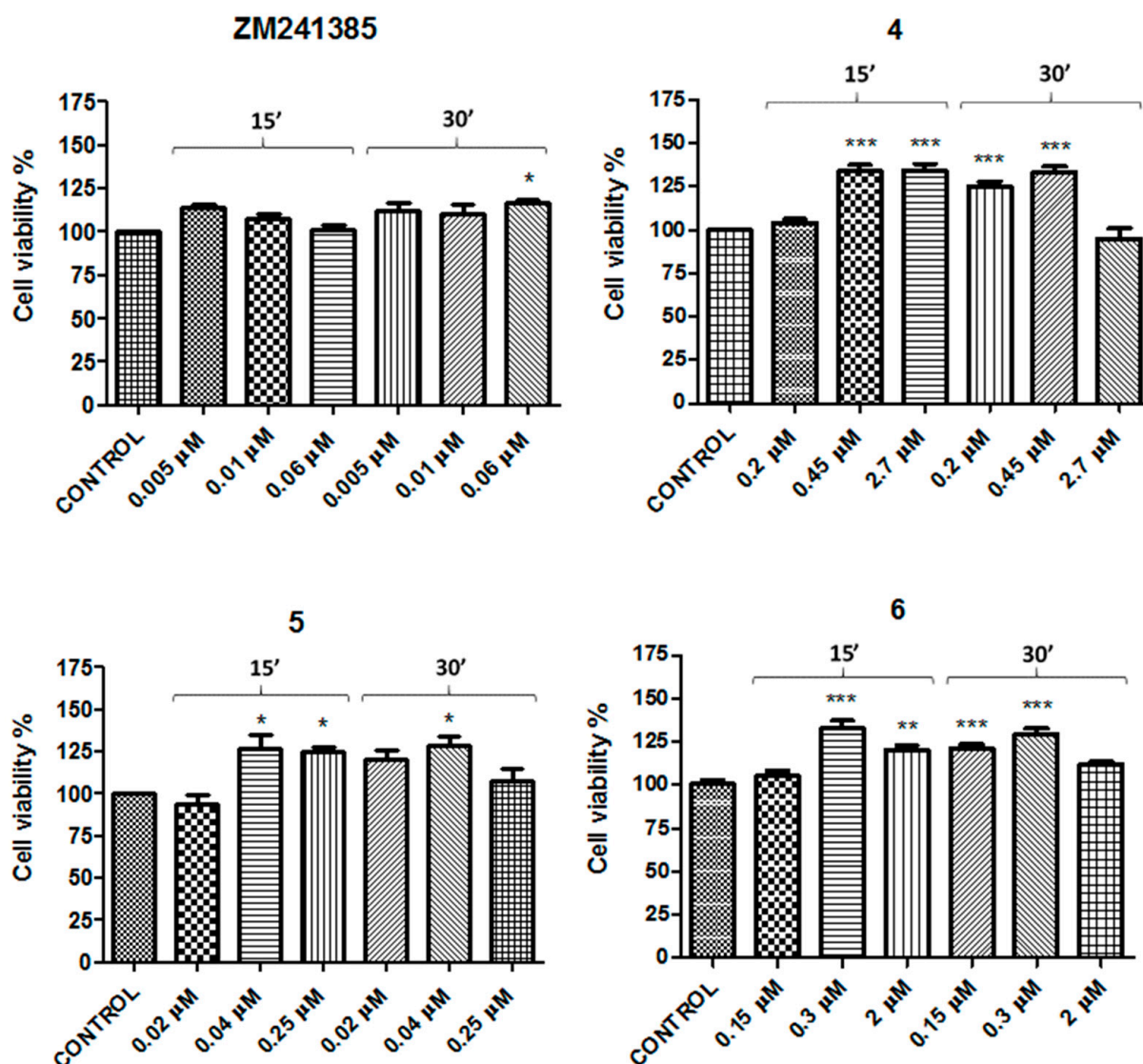


**Figure 3.** Effects of ZM241385 and compounds 4–6 on N13 cells. Percentage of cell viability after treatment with different ligand concentrations for 15 or 30 min of incubation. Results represent the average of 3–5 independent experiments. \*  $p < 0.05$ , \*\*  $p < 0.01$ , \*\*\*  $p < 0.001$  (one-way ANOVA followed by Dunnett's multiple comparison test of treated cells against control).

In order to verify if these compounds could provide protection in an in vitro inflammatory model, the N13 cell cultures were exposed to a pro-inflammatory cocktail of cytokines (CK) constituted by TNF- $\alpha$ , IL-1 $\beta$ , and IFN- $\gamma$  20 ng/mL for 48 h. The results showed that this inflammatory insult decreased cell viability in a significative mode (35%  $\pm$  3 vs. control). The experiments in the presence of compounds 1–3 and CCPA were performed by pretreating cells with these compounds at the same concentration utilized in precedent experiments (Table 3), 30 min before adding the CK cocktail for 48 h. Results reported in Figure 4 demonstrate that these compounds were able to prevent the damage induced by the CK cocktail as well as CCPA (Figure 4). The best effect was shown by compound 1 at 8  $\mu$ M after 30 min of incubation (149%  $\pm$  3.5 vs. CK).

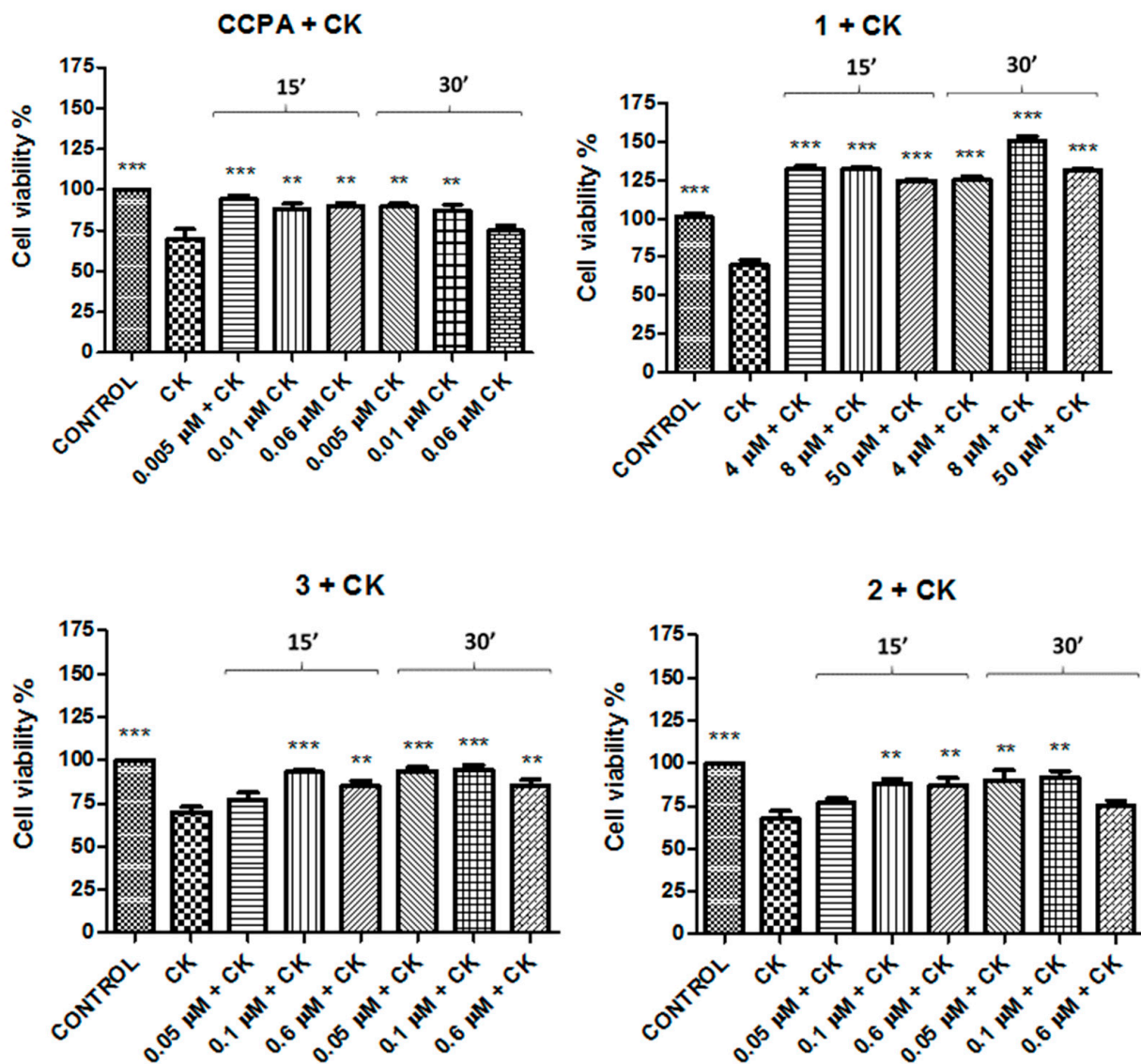


**Figure 4.** Protective effects of CCPA and compounds 1–3 against cytokine (CK) aggression on N13 cells. Percentage of cell viability after treatment with the CK cocktail for 48 h. Results represent the average of 3–5 independent experiments. \*\*  $p < 0.01$ , \*\*\*  $p < 0.001$  (one-way ANOVA followed by Dunnett's multiple comparison test of treated cells against CK).

In addition, since, in neuroinflammation, there is an overexpression of  $A_{2A}AR$ , the experiments with  $A_{2A}AR$  antagonists were performed by pretreating cells with 20 ng/mL of CK cocktail for 48 h and then with compounds 4–6 or the referent compound ZM241385 at the same concentration used in cell viability for 15, 30 min (Table 3). The results reported in Figure 5 exhibit that the best effect was obtained by compound 6 at 0.3  $\mu$ M after 30 min of incubation (157%  $\pm$  3.2 vs. CK).

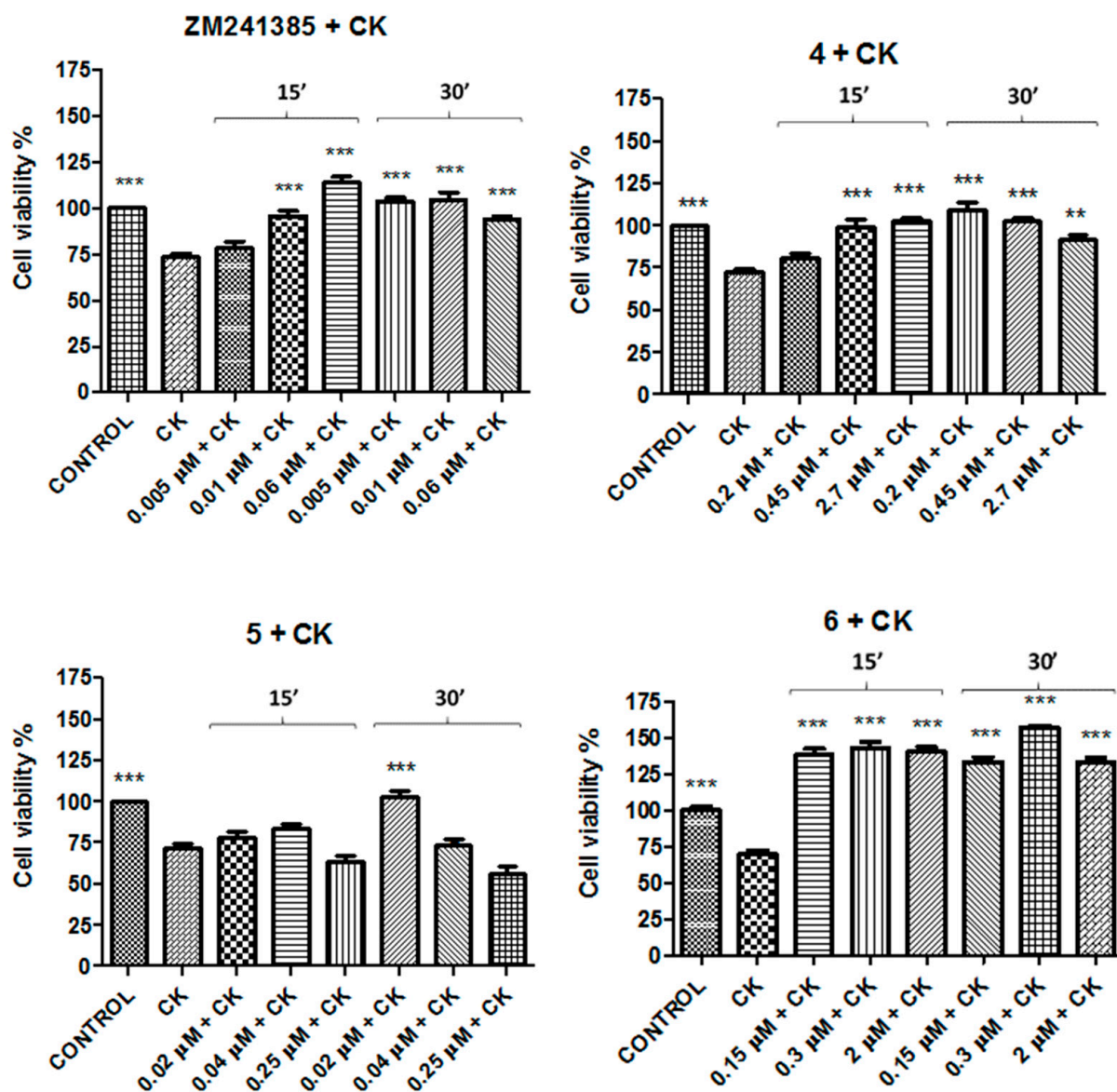


**Figure 5.** Restoring effects of ZM241385 and compounds 4–6 against CK aggression on N13 cells. Results represent the average of 3–5 independent experiments. \*\*  $p < 0.01$ , \*\*\*  $p < 0.001$  (one-way ANOVA followed by Dunnett’s multiple comparison test of treated cells against CK).

To confirm the results obtained, the two most active compounds (1 and 6) were studied using a second cell viability assay based on the quantification of ATP produced by live cells. Experiments were performed according to the procedure carried out with CellTiter 96<sup>®</sup> AQueous One Solution Cell Proliferation Assay. It was observed that the effects obtained by compounds 1 and 6 were comparable with those detected in the other cell viability assay at 8 and 0.3  $\mu$ M after 30 min of incubation ( $145\% \pm 4.2$  vs. CK and  $152\% \pm 4.6$  vs. CK, respectively, Figure 6).



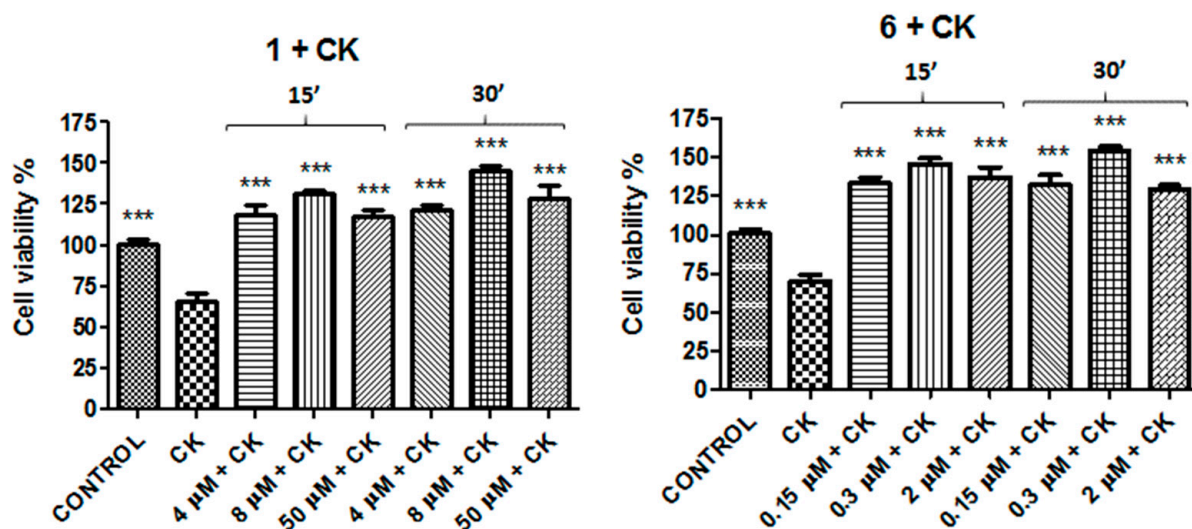


**Figure 6.** Protective (compound 1) or restoring (compound 6) effects after or before incubation of cells with CK. Bar graphs presents the percentage cell viability, and results are presented as the average of 3–5 independent experiments. \*\*\*  $p < 0.001$  (one-way ANOVA followed by Dunnett's multiple comparison test of treated cells against CK).

Since compounds 1 and 6 were shown to be the best compounds to prevent or counteract the effect of CK cocktail, parallel experiments were performed treating, for 30 min, N13 cells with a selective  $A_1$ AR antagonist, DPCPX (1,3-Dipropyl-8-cyclopentylxanthine), and a selective  $A_{2A}$ AR agonist, CGS21680 (2-(4-(2-Carboxyethyl)phenethylamino)-5'-*N*-ethylcarboxamidoadenosine), in combination with compounds 1 and 6 or reference compounds CCPA and ZM241385, respectively, in order to verify the involvement of these receptors in obtained results. The results are reported in Figure 7.

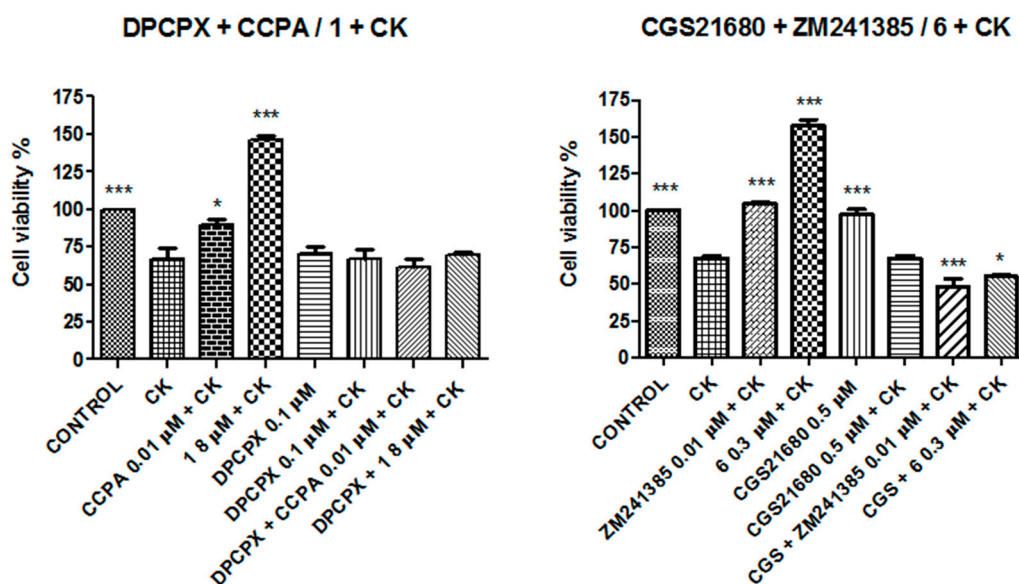


**Figure 7.** Co-incubation of N13 cells with the  $A_1$ AR antagonist DPCPX and the selective  $A_{2A}$ AR agonist CGS21680 in combination with compounds 1 and 6 or CCPA and ZM241385, respectively. \*  $p < 0.05$ , \*\*\*  $p < 0.001$  (one-way ANOVA followed by Dunnett's multiple comparison test of treated cells against CK).

At this point, a further study was performed to elucidate a possible synergic effect between compounds 1 and 6 and reference compounds CCPA and ZM241385 to contrast the damage produced by the CK cocktail. Experiments in combination were performed

using 8  $\mu\text{M}$  for compound **1**, 0.3  $\mu\text{M}$  for compound **6**, and 0.01  $\mu\text{M}$  for CCPA and ZM241385 after 30 min of incubation. The same experiments were also performed in the presence of the CK cocktail (Figure 8).

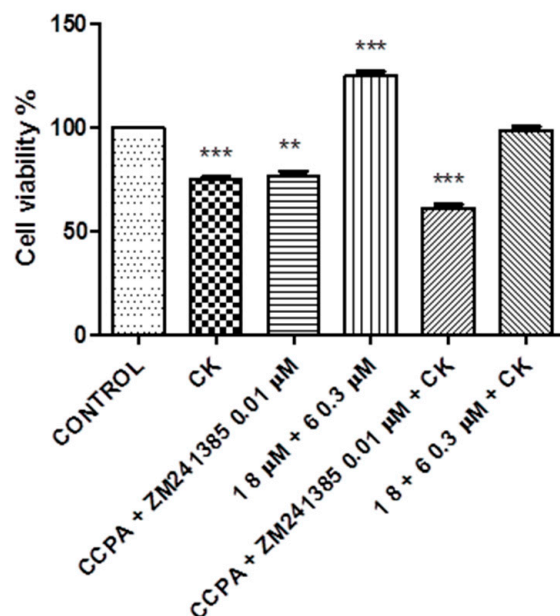


**Figure 8.** Co-incubation of N13 cells with compounds **1** and **6** or with reference compounds CCPA and ZM241385. Results represent the average of 3–5 independent experiments. \*\*  $p < 0.01$ , \*\*\*  $p < 0.001$  (one-way ANOVA followed by Dunnett’s multiple comparison test of treated cells against control).

In addition, the same experiment was repeated at lower doses—compound **1** at 0.4  $\mu\text{M}$  and compound **6** at 0.15  $\mu\text{M}$ . The results are reported in Figure 9.

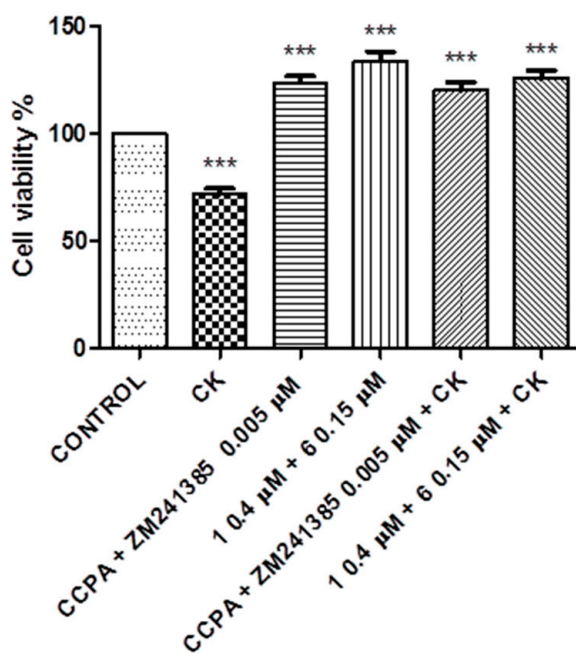


**Figure 9.** Co-incubation of N13 cells with compounds **1** and **6** or with reference compounds CCPA and ZM241385. Results represent the average of 3–5 independent experiments. \*\*\*  $p < 0.001$  (one-way ANOVA followed by Dunnett’s multiple comparison test of treated cells against control).

A Hoechst assay was performed to verify the anti-apoptotic properties of compounds **1** and **6**. Image analysis revealed a significant decrease in cell circularity and area detected in cells treated with the CK cocktail compared to control cells ( $p$ -values < 0.05) (Figures 10 and 11). This decrease was assumed to indicate DNA degradation. The results correlate positively and significantly with those obtained by cell viability assay ( $R = 0.989$ ,  $p$ -value < 0.05).

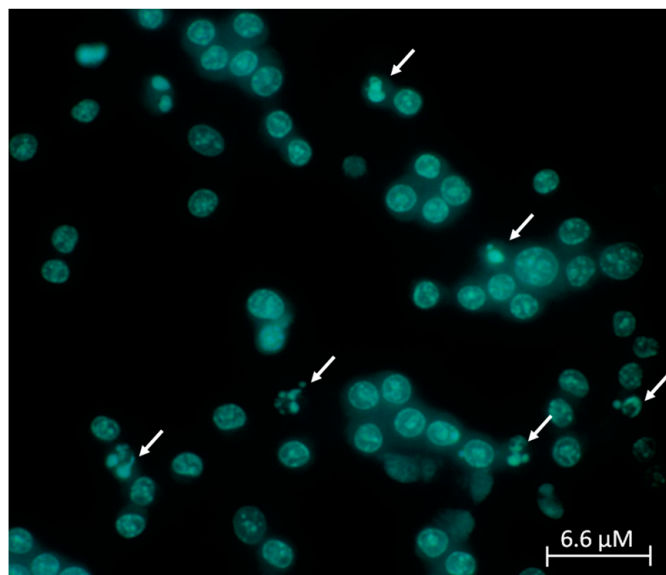


**Figure 10.** Example of an image obtained through Hoechst assay. In the picture, arrows point to apoptotic cells (40× magnification).

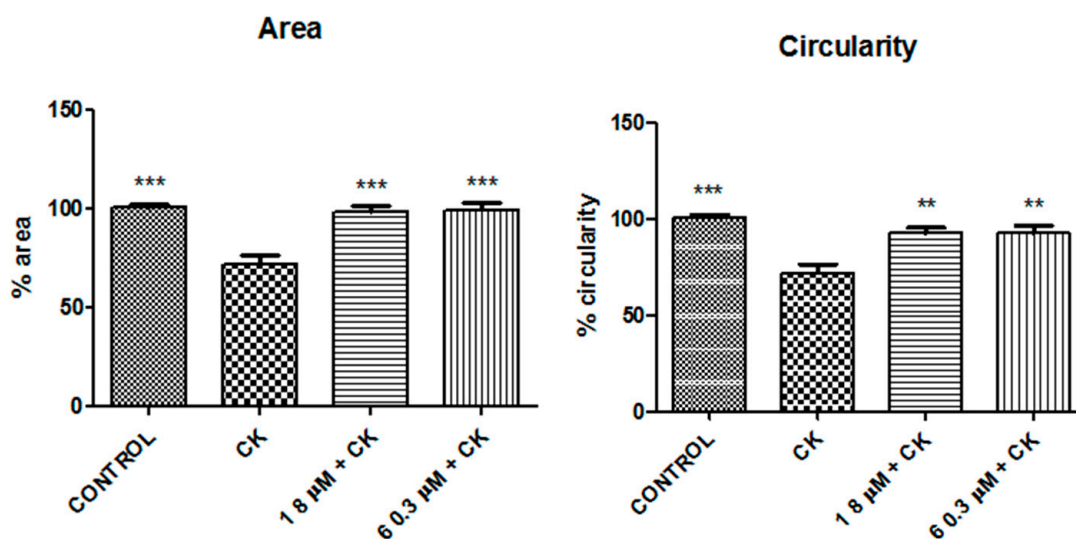


**Figure 11.** Cell area and circularity after the pre- and post-treatment with compound **1** and compound **6**, respectively, in presence of the CK cocktail. Results represent the average of three independent experiments. \*\*  $p < 0.01$ , \*\*\*  $p < 0.001$  (one-way ANOVA followed by Dunnett's multiple comparison test of treated cells against CK).

Effects obtained with compounds **1** and **6** after 30 min of incubation indicated that they have a protective effect and contrast the CK aggression in a statistically significant way, demonstrating that they have anti-apoptotic properties (Figure 11).

To confirm the anti-apoptotic properties of compounds **1** and **6**, the Annexin V/PI test was performed. The percentage of apoptotic cells was calculated based on the results of cellular staining. Apoptotic cells were Annexin V-FITC-positive/PI-negative and both An-

nexin V-FITC/PI-positive. They appeared green (Annexin V-FITC staining), while necrotic cells appeared red (PI staining) and apo-necrotic cells light orange (Figure 12). Compounds 1 and 6 were incubated at concentrations of 8 and 0.3  $\mu\text{M}$ , respectively. Generally, the anti-apoptotic effect was observed with both compounds and the percentages of apoptotic cells were similar. In Figure 12 (panel 1) are reported the results obtained with compound 1 as example. The percentage of apoptotic cells treated with compounds 1 and 6 was 19% and 21%, respectively, followed by 45% in CK cocktail treatment and 11% and 12% in untreated cells and cells treated with solvent, respectively (Figure 12 panel 2).

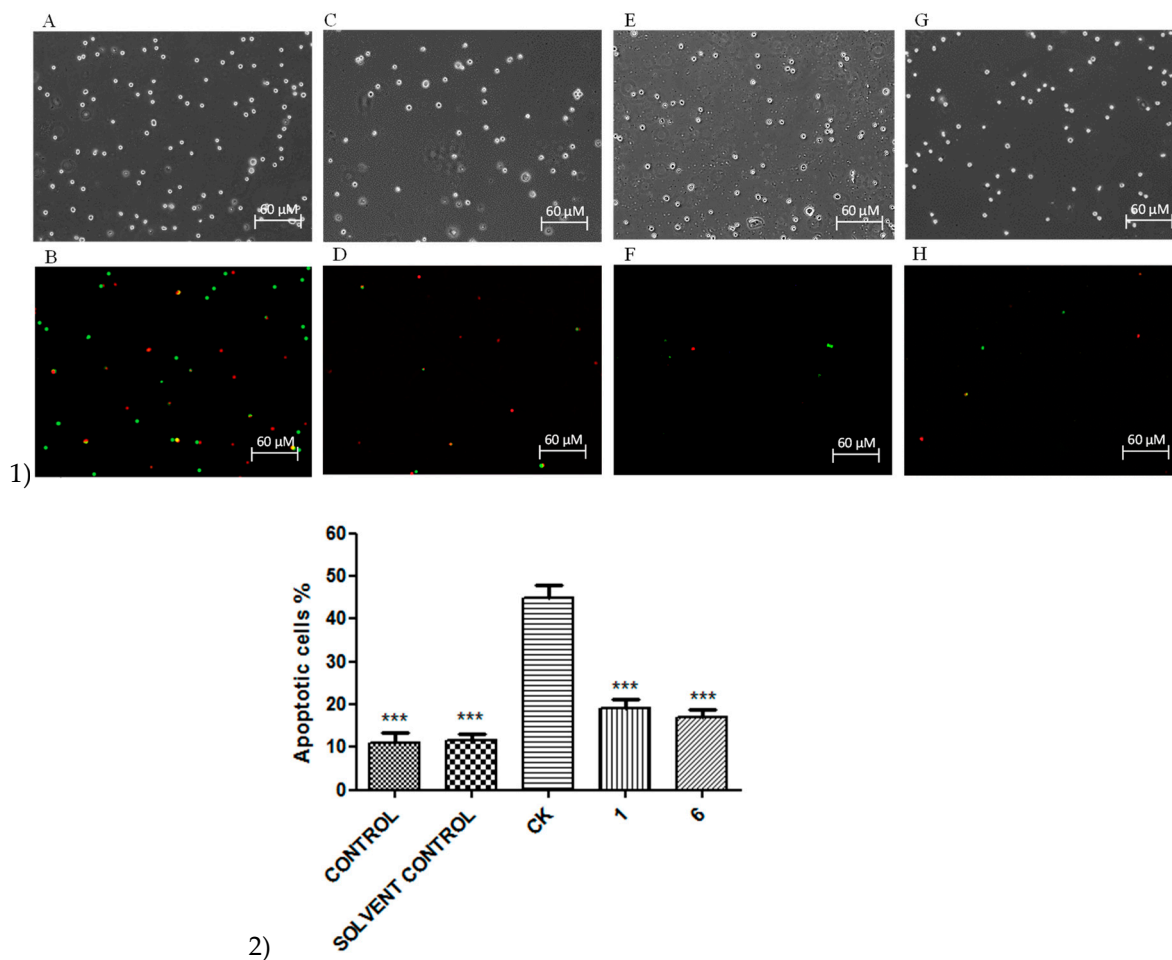


**Figure 12.** (1) Annexin V/PI double staining assay of N13 cells treated for 48 h with CK cocktail (A,B) and CK cocktail plus compound 1 (C,D) in comparison with untreated control (E,F) and solvent control (G,H). Each group of pictures (10 $\times$  magnification) is composed of contrast phase and fluorescence images, which underline the anti-apoptotic effect of compound 1. (2) Percentage of apoptotic cells after treatment with CK cocktail or CK plus compound 1 or 6, in comparison with the untreated control and solvent control. Each bar represents mean  $\pm$  S.E. \*\*\*  $p < 0.001$  (one-way ANOVA followed by Dunnett's multiple comparison test of treated cells or controls against CK).

### 3. Discussion

The present study provides evidence for the involvement of  $A_1\text{AR}$  and  $A_{2A}\text{AR}$  in neuroinflammation regulation. Neuroinflammation is a pathological state of inflammatory responses localized in the brain and spinal cord. Since chronic neuroinflammation is correlated to neurodegeneration, there is a significant interest in understanding the mechanisms involved in inflammatory responses [32]. Microglia are the principal cells involved in innate immune surveillance and their activation is key in neuroinflammation. These myeloid cells express ARs and it is well known that total expression of  $A_1\text{AR}$  and  $A_{2A}\text{AR}$  changes after aggression. Indeed, there are many research findings [33–35] that



have reported the changes in ARs; in particular, A<sub>1</sub>AR is downregulated and A<sub>2A</sub>AR upregulated after an insult. This work was carried out starting from this evidence using full and partial agonists to stimulate the A<sub>1</sub>AR and antagonists to block the A<sub>2A</sub>AR in *in vitro* models of neuroinflammation. Immunostaining experiments were performed in order to verify the presence of A<sub>1</sub>AR and A<sub>2A</sub>AR in N13 cells, which are essential to exclude false negative and/or positive results. The presence of A<sub>1</sub>AR and A<sub>2A</sub>AR was confirmed by the double immunofluorescence staining of N13 cell cultures in the presence of adenosine A<sub>1</sub> receptor polyclonal antibody Alexa Fluor<sup>®</sup> 488-conjugated and adenosine A<sub>2A</sub> receptor antibody Alexa Fluor<sup>®</sup> 594-conjugated. A pilot cell viability experiment was performed up to 72 h, but since there was no difference with respect to 30 min, the experimental time choice was 30 min. The results of cell viability proved that the reference compounds CCPA and ZM241385 were able to increase cell viability with respect to the control, and the maximum effect was observed at 0.005 μM (139% ± 4.6 and 119% ± 3.4 vs. control, respectively) after 30 min of incubation (Figures 2 and 3). All of the A<sub>1</sub>AR agonists and A<sub>2A</sub>AR antagonists exhibited very similar results (Figures 2 and 3), demonstrating a non-toxic effect. Experiments carried out up to 72 h showed only a non-significant decrease ( $p < 0.05$ ) in cell viability, confirming a non-toxic profile also after a long exposure.

Activated microglia release some cyto-/chemokine-based signals, especially during emergencies, representing a rich and instant brain endogenous source for numerous cyto- and chemokines. Cytokines constitute a significant portion of the immuno- and neuro-modulatory messengers that can be released during microglia activation. However, excessive or sustained activation significantly contributes to acute and chronic neuropathologies. Dysregulation of microglial cytokine production promotes harmful actions of the defense mechanisms, resulting in direct neurotoxicity. For these reasons, the experiments were performed in presence of a CK cocktail in order to reproduce the induced neurotoxicity. These experiments were performed taking into account the different expression levels of A<sub>1</sub>AR and A<sub>2A</sub>AR during neuroinflammatory pathologies. The decrease in A<sub>1</sub>AR in microglia, macrophages, and neurons leads to a state of neuroinflammation and the activation of A<sub>1</sub>AR leads to neuroprotective effects [36–40]. On the other hand, overexpression of A<sub>2A</sub>AR is associated to chronic stress and A<sub>2A</sub>AR stimulation is involved in neurodegeneration [41,42]. On these bases, the experiments with A<sub>1</sub>AR agonists were performed using compounds before the insult with CKs, and they were present during and after the inflammatory insults for the entire experiment duration. On the contrary, A<sub>2A</sub>AR antagonists were administered after the aggression with the CK cocktail in order to decrease the upregulation induced. The reported results demonstrate that this strategy is accurate; in fact, the administration of agonists before the CK insult completely prevented the aggression and the antagonists after CK counteracted the damage effect of them as well as CCPA and ZM241385, respectively. The same experiments were performed with another cell viability assay based on the quantification of ATP produced by live cells to corroborate the results. The best results, in both cell viability assays, were obtained with the agonist compound 1 at 8 μM and the antagonist compound 6 at 0.03 μM, both after 30 min of incubation. For this reason, these two compounds were chosen for further experiments. It is worthwhile to note that compound 1 is a partial A<sub>1</sub>AR agonist and this produces a desired submaximal response, avoiding the overstimulation of receptors [43]. Furthermore, note that desensitization of G protein-coupled receptors (GPCRs), such as A<sub>1</sub>AR, is activated almost simultaneously with their activation. Partial agonists produce agonist-dependent receptor phosphorylation decreased by protein-coupled receptor kinase G (GRK) with a reduction in desensitization consequent to a prolongation of activation and fewer side effects [44].

After the inflammatory insult, a significant increase in cell viability was observed both with compounds 1 and 6. The treatment with compound 1 at 8 μM for 30 min produced an increase in cell viability of 149%. A similar result was observed with compound 6 at 0.3 μM (157 %) for 30 min of incubation (Figures 3 and 4). The effect of the cell viability increase produced by compounds 1 and 6, alone and in the presence of the CK insult, after 30 min

is imputable both to increased cell proliferation and to an increase in cellular metabolic processes. This assertion was confirmed by results obtained with trypan blue experiments that allowed quantifying the cell proliferation.

The experiments performed with DPCPX, a selective A<sub>1</sub>AR antagonist, and CGS21680, a selective A<sub>2A</sub>AR agonist, in combination with compounds **1** and **6** or with reference compounds CCPA and ZM241385 demonstrated that the addition of DPCPX produces cell damage similarly to the CK cocktail, and co-incubation with compound **1** or CCPA did not ameliorate the cell viability. In fact, it is clear that DPCPX antagonized the effects of both CCPA and compound **1** since, in its presence, there was not a recovery in decreased cell survival produced by the CKs (150%). On the other hand, incubation with the A<sub>2A</sub>AR agonist CGS21680 did not produce a decrease in cell viability, but at the same time, it did not counteract the effect of the CK cocktail. In addition, co-incubation with CGS21680 and ZM241385 or compound **6** did not produce any increase in cell viability with respect to the CK cocktail. In conclusion, these experiments confirmed the involvement of A<sub>1</sub>AR and A<sub>2A</sub>AR in the effects produced by compounds **1** and **6**, respectively.

These results underline the ability of these compounds, by A<sub>1</sub>AR and A<sub>2A</sub>AR interaction, to prevent, in vitro, microglial death and promote microglial growth. Further studies are planned to verify if these actions will be confirmed in vivo.

The best efficacy is often obtained with combination therapies that produce a decrease in toxicity and a reduced development of drug resistance. Combination therapies have become a standard for the treatment of several diseases, continuing to feature a promising approach in indications where a single treatment is doomed to failure [45–48]. In this context, since the A<sub>1</sub>AR agonist and A<sub>2A</sub>AR antagonist counteract the neuroinflammation produced by a CK cocktail, co-administration of these ligands could bring an increased benefit against it. The experiment performed using a combination with compounds **1** and **6** and the compounds CCPA and ZM241385 showed that there was not an additive effect when administering couples of compounds in combination, but it is interesting to note that compounds **1** and **6** were demonstrated to be much more effective in counteracting CK damage than the reference compounds (Figure 8). This result is probably imputable to the dose effect-based approaches; in fact, the dose that produced the maximum effect of each compound was used. For this reason, further experiments were performed with a combination of sub-threshold doses. The non-effective doses of compounds **1** and **6** or CCPA and ZM241385 produced a significant ( $p < 0.005$ ) increased effect in combination compared to the maximum dose of each compound (Figure 9). Compounds **1** and **6** demonstrated, in this case also, to be more effective in counteracting CK damage than the reference compounds. This finding provides new opportunities for the rational development of combination therapies in neuroinflammation, limiting side effects.

In recent years, there have been many papers regarding tests about the study of the well-known A<sub>1</sub>AR agonist CCPA and A<sub>2A</sub>AR antagonists SCH 58261 (2-(2-Furanyl)-7-(2-phenylethyl)-7H-pyrazolo[4,3-e][1,2,4]triazolo[1,5-c]pyrimidin-5-amine) and ZM241385 in neurodegenerative disorders, both in cells and animal models. On the contrary, until now, there is no evidence about the use of A<sub>1</sub>AR partial agonists and A<sub>2A</sub>AR antagonists in therapeutic approaches used in combination. Since an emerging anti-neurodegenerative role for prolonged A<sub>1</sub>AR activation and A<sub>2A</sub>AR inhibition could represent a targeted strategy in multiple neurodegenerative diseases such as Alzheimer's, Parkinson's, and multiple sclerosis, the combination of A<sub>1</sub>AR partial agonists and A<sub>2A</sub>AR antagonists represents a future prospect for the treatment of these pathologies [35,49–55].

In recent years, various studies demonstrated that the secretion of cytokines by microglia activation induces the activation of two distinct pathways, apoptosis and nuclear factor kappa-light-chain-enhancer of activated B cells (NF-κB) [49,56]. In order to verify the anaprotic effect of compounds **1** and **6**, two experiments, a Hoechst assay and an Annexin V-FITC test, were performed.

The Hoechst assay was performed in order to verify if the cell circularity and area were influenced by the CK cocktail and by compounds **1** and **6**. After treatment with

the CK cocktail, there was a significant decrease in cell circularity and area, and this indicates possible DNA degradation, but after treatment with compounds **1** and **6**, there was a protective effect and a contrast to CK aggression in a statistically significant way, demonstrating the anti-apoptotic properties of these compounds (Figure 11). Further confirmation was obtained by the Annexin V-FITC test in combination with propidium iodide that is able to differentiate between apoptosis and necrosis. In fact, the Annexin V permitted the identification of viable, transient apoptotic and necrotic cells, since cells undergoing apoptosis or necrosis have clearly distinct morphological features. In the early apoptosis stages, exposure to phosphatidylserine (PS) on cell surface occurs, followed by membrane blebbing, nuclear fragmentation, decreased cell volume, and formation of apoptotic bodies. On the other hand, programmed necrosis morphological features include early plasma membrane rupture and rapid cytoplasmic and nuclear swelling [57]. For these reasons, apoptotic-like cell death is often quantified by measuring PS externalization by binding of Annexin V.

Apoptotic Annexin V-positive cells were confirmed by microscopical analysis in comparison to untreated N13 cells. These studies provide evidence that chromatin condensation coincides with exposure to CK cocktail. In fact, as shown in Figure 12A,B, after CK cocktail exposure, it is possible to evaluate, by Annexin V/PI staining, double-positive late apoptotic cells and necrotic cells in an amount of 45% in CK cocktail treatment, and 11% in untreated cells (Figure 12G,H). On the other hand, in the presence of compounds **1** and **6**, the amount of double-positive late apoptotic cells and necrotic cells was greatly reduced (Figure 12C–F) to a percentage of 19% and 21%, respectively. This experiment confirmed the results obtained with the Hoechst assay, demonstrating that compounds **1** and **6** possess good anti-apoptotic properties.

#### 4. Materials and Methods

Compounds **1–6** were synthesized at the School of Pharmacy of Camerino University (Italy) and dissolved in dimethyl sulfoxide (DMSO) to prepare a 10-mM stock solution, which was then diluted with water to the concentration required for the experiments. In all experiments, the maximum concentration of DMSO in wells did not exceed 0.5% and had no effect on cell viability. CCPA, ZM241385, CGS21680, DPCPX, and Hoechst 33258 were purchased from Sigma-Aldrich (Milan, Italy). All materials concerning cell culture were purchased from EuroClone S.p.A. (Milan, Italy); CellTiter 96<sup>®</sup> AQueous One Solution Cell Proliferation and CellTiter-Glo<sup>®</sup> Luminescent Cell Viability Assays were purchased from Promega (Milan, Italy). The Annexin V-FITC Apoptosis Detection Kit (BioVision) was bought from DBA S.r.L. (Milan, Italy).

##### 4.1. Cells Culture

N13 cells were grown in DMEM (Dulbecco's Modified Eagle Medium) High Glucose supplemented with 10% fetal bovine serum, 100 U/mL penicillin, 100 µg/mL streptomycin, 1 mM sodium pyruvate, and 2 mM L-glutamine in a humidified atmosphere with 5% CO<sub>2</sub> at 37 °C. Compounds were dissolved in DMSO to have a final concentration of 10 mM and, prior to use, were then diluted with water.

##### 4.2. Immunocytochemistry

A<sub>1</sub>AR and A<sub>2A</sub>AR presence was investigated using an immunofluorescence technique. A<sub>1</sub>AR presence was checked using the adenosine A<sub>1</sub> receptor polyclonal antibody Alexa Fluor<sup>®</sup> 488-conjugated, while A<sub>2A</sub>AR was studied by adenosine A<sub>2A</sub> receptor antibody Alexa Fluor<sup>®</sup> 594-conjugated. Briefly, media were aspirated and cells fixed with Fixative Solution for 15 min (high-purity 4% formaldehyde in PBS (Phosphate Buffered Saline), pH = 7.3). After that, they were washed 3 times with PBS and permeabilized with a Permeabilization Solution (0.5% Triton X-100) for 15 min [58]. They were washed again with PBS and incubated for 1 h with Blocking Buffer (3% BSA (Bovine Serum Albumin),

fraction V delipidated in PBS). Finally, antibody labeling proceeded and cells were seeded in a 6-well plate at  $3 \times 10^5$  cells per well.

#### 4.3. Trypan Blue Exclusion Test

Briefly,  $3 \times 10^5$  N13 cells were seeded in a six-well plate and incubated for 24 h. Subsequently, compounds 1 and 6 were added at a concentration of 8 and 0.3  $\mu$ M, respectively, in the absence or presence of a CK cocktail. After the incubation, cells were detached with Trypsin-EDTA solution and centrifuged at 1200 rpm for 10 min. Cell viability was determined using trypan blue staining, using a Countess II Automated Cell Counter (Thermo Fisher Scientific, USA) to count the number of live and dead cells.

#### 4.4. Cell Titer 96<sup>®</sup> AQueous One Solution Cell Proliferation Assay

Briefly,  $1 \times 10^4$  N13 cells were plated in 98  $\mu$ L medium and incubated in a 96-well plate overnight. After 24 h, 2  $\mu$ L ligand or CK cocktail was added to the wells. After treatment, 20  $\mu$ L CellTiter 96<sup>®</sup> AQueous One Solution Reagent was added in each well and allowed to incubate for 1 h [59]. Absorbance was measured at 492 nm in a microplate reader. Cell viability was calculated as a percentage using the formula: (mean OD (Optical Density) of treated cells/mean OD of control cells)  $\times$  100. Results were expressed as percentage of control cells that were not treated. An untreated control and a control with the solvent were run. All experiments were performed in triplicate.

#### 4.5. CellTiter-Glo<sup>®</sup> Luminescent Cell Viability Assay

Briefly,  $1 \times 10^4$  N13 cells were seeded into 96-well cell culture plates and incubated overnight. After 24 h, 2  $\mu$ L ligand or CK cocktail was added to the wells. After treatment, cells were lysed using CellTiter Glo reagent, and the luminescence signals produced by ATP molecules from metabolically active cells were measured using a plate reader after 30 min incubation at room temperature. Results were expressed as percentage of control cells that were not treated. An untreated control and a control with the solvent were run. All experiments were performed in triplicate.

#### 4.6. Hoechst Assay

A Hoechst assay was carried out to check the anti-apoptotic effect of the understudy compounds using Hoechst 33258. Briefly,  $3 \times 10^5$  N13 cells were seeded in a six-well plate. After 24 h, the media were eliminated and cells washed with PBS. Then, they were washed with acetic acid/methanol solution 50:50, washed again with PBS, and incubated for 10 min with a fixative solution. After this, cells were cleaned with distilled water and incubated light-protected for 30 min at rt with Hoechst (1  $\mu$ g/mL). Finally, the dye was discarded and cells were washed with water. Glycerol solution was added and cells were observed under an Olympus microscope. The cell area and circularity were measured using ImageJ as the image analyzing software [60]. Area and circularity were calculated as percentages using the following formula:

$$\text{Area or circularity} = \frac{\text{area or circularity of treated cells}}{\text{area or circularity of control cells}} \times 100$$

#### 4.7. Apoptosis and Necrosis Assay

The Annexin V-FITC test was performed to evaluate the anti-apoptotic effect of understudy compounds thanks to the capability of the kit to differentiate between apoptosis and necrosis. Briefly,  $3 \times 10^5$  N13 cells were seeded in a six-well plate. After 24 h, the media were eliminated and cells were washed with PBS and centrifuged. The pellet was resuspended with 500  $\mu$ L binding buffer and 5  $\mu$ L Annexin V-FITC and 5  $\mu$ L propidium iodide were added. The mix was incubated at room temperature for 5 min in the dark. Cell suspension was added on a glass slide and covered with a glass coverslip, and then, the glass slide was monitored with a fluorescence microscope coupled to a cell imaging system,



using a dual filter set for FITC and rhodamine [61]. Approximately 300 cells were used for each analysis. Results are the mean of three different experiments.

#### 4.8. Statistical Analysis

Quantitative data are presented as means  $\pm$  SE from 3–5 independent experiments. The significance of differences was evaluated using a two-tailed Student's *t*-test or one-way ANOVA followed by Dunnett's post-test. Statistical analysis was carried out with GraphPad Prism8 Software (San Diego, CA, USA).  $p \leq 0.05$  were considered as statistically significant.

### 5. Conclusions

Existing evidence indicates that chronic inflammation mediated by the activation of microglia plays a significant role in neurodegenerative diseases. A<sub>1</sub>AR is considered a neuroprotective receptor, and A<sub>2A</sub>AR is designated as a neurodegenerative receptor; therefore, A<sub>1</sub>AR stimulation and A<sub>2A</sub>AR inhibition could be one of the most promising strategies to treat neurodegenerative diseases. The aim of this work was to elucidate the role of these receptors in neuroinflammation modulation using potent and selective A<sub>1</sub>AR agonists and A<sub>2A</sub>AR antagonists. Among the studied ligands, compounds **1** and **6** were found to be particularly active in counteracting CK damage, even more than the reference compounds, and it was proven that the effect exerted was due to the interaction with A<sub>1</sub>AR and A<sub>2A</sub>AR. Moreover, since the two compounds have shown a synergistic effect in counteracting the apoptotic effect induced by CK, they could represent a promising approach for the therapy of neurodegenerative diseases in which a single treatment is doomed to failure.

**Author Contributions:** Conceptualization and design: G.M. and M.B.; methodology and investigation: M.B. and A.M.N.; formal analysis: M.B., A.S., C.L., and D.D.B.; resources: M.B.; writing—original draft preparation: G.M. and M.B.; supervision: G.M. and R.V.; project administration: G.M. All authors have read and agreed to the published version of the manuscript.

**Funding:** This research was supported by the University of Camerino, Fondo di Ricerca di Ateneo (FPI000065 FAR 2019).

**Data Availability Statement:** No new data were created or analyzed in this study.

**Conflicts of Interest:** The authors declare no conflict of interest.

**Sample Availability:** Samples of the compounds are available from the authors.

### References

1. Pelvig, D.P.; Pakkenberg, H.; Stark, A.K.; Pakkenberg, B. Neocortical glial cell numbers in human brains. *Neurobiol. Aging* **2008**, *29*, 1754–1762. [[CrossRef](#)] [[PubMed](#)]
2. Verkhratsky, A.; Nedergaard, M. Physiology of Astroglia. *Physiol. Rev.* **2018**, *98*, 239–389. [[CrossRef](#)] [[PubMed](#)]
3. Perry, V.H.; Cunningham, C.; Holmes, C. Systemic infections and inflammation affect chronic neurodegeneration. *Nat. Rev.* **2007**, *7*, 161–167. [[CrossRef](#)]
4. Streit, W.J.; Mrak, R.E.; Griffin, W.S. Microglia and neuroinflammation: A pathological perspective. *J. Neuroinflamm.* **2004**, *1*, 14. [[CrossRef](#)] [[PubMed](#)]
5. Hanisch, U.K.; Kettenmann, H. Microglia: Active sensor and versatile effector cells in the normal and pathologic brain. *Nat. Neurosci.* **2007**, *10*, 1387–1394. [[CrossRef](#)]
6. Davalos, D.; Grutzendler, J.; Yang, G.; Kim, J.V.; Zuo, Y.; Jung, S.; Littman, D.R.; Dustin, M.L.; Gan, W.B. ATP mediates rapid microglia response to local brain injury in vivo. *Nat. Neurosci.* **2005**, *8*, 752–758. [[CrossRef](#)]
7. Koizumi, S.; Shigemoto-Mogami, Y.; Nasu-Tada, K.; Shinozaki, Y.; Ohsawa, K.; Tsuda, M.; Joshi, B.V.; Jacobson, K.A.; Kohsaka, S.; Inoue, K. UDP acting at P2Y6 receptors is a mediator of microglia phagocytosis. *Nature* **2007**, *446*, 1091–1095. [[CrossRef](#)]
8. Boison, D. Adenosine as a modulator of brain activity. *Drug News Perspect.* **2007**, *20*, 607–611. [[CrossRef](#)] [[PubMed](#)]
9. Schmidt, J.; Ferk, P. Safety issues of compounds acting on adenosinergic signalling. *J. Pharm. Pharmacol.* **2017**, *69*, 790–806. [[CrossRef](#)] [[PubMed](#)]
10. Sebastiao, A.M.; Ribeiro, J.A. Fine-tuning neuromodulation by adenosine. *Trends Pharmacol. Sci.* **2000**, *21*, 341–346. [[CrossRef](#)]
11. Sebastiao, A.M.; Ribeiro, J.A. Adenosine receptors and the central nervous system. *Handb. Exp. Pharmacol.* **2009**, *193*, 471–534.
12. De Mendonca, A.; Ribeiro, J.A. Adenosine and synaptic plasticity. *Drug Dev. Res.* **2001**, *52*, 283–290. [[CrossRef](#)]

13. Stone, T.W.; Ceruti, S.; Abbracchio, M.P. Adenosine receptors and neurological disease: Neuroprotection and neurodegeneration. *Handb. Exp. Pharmacol.* **2009**, *193*, 535–587.
14. Stockwell, J.; Jakova, E.; Cayabyab, F.S. Adenosine A1 and A2A receptors in the brain: Current research and their role in neurodegeneration. *Molecules* **2017**, *22*, 676. [[CrossRef](#)] [[PubMed](#)]
15. Luongo, L.; Guida, F.; Imperatore, R.; Napolitano, F.; Gatta, L.; Cristino, L.; Giordano, C.; Siniscalco, D.; Di Marzo, V.; Bellini, G.; et al. The A1 adenosine receptor as a new player in microglia physiology. *Glia* **2014**, *62*, 122–132. [[CrossRef](#)] [[PubMed](#)]
16. Blackburn, M.R.; Vance, C.O.; Morschl, E.; Wilson, C.N. Adenosine receptors and inflammation. In *Adenosine Receptors in Health and Disease*; Wilson, C.N., Mustafa, S.J., Eds.; Springer: Berlin/Heidelberg, Germany, 2009; Volume 193, pp. 215–269.
17. Cronstein, B.N.; Levin, R.I.; Philips, M.; Hirschhorn, R.; Abramson, S.B.; Weissmann, G. Neutrophil adherence to endothelium is enhanced via adenosine A1 receptors and inhibited via adenosine A2 receptors. *J. Immunol.* **1992**, *148*, 2201–2206.
18. Zahler, S.; Becker, B.F.; Raschke, P.; Gerlach, E. Stimulation of endothelial adenosine A1 receptors enhances adhesion of neutrophils in the intact guinea pig coronary system. *Cardiovasc. Res.* **1994**, *28*, 1366–1372. [[CrossRef](#)] [[PubMed](#)]
19. Lambertucci, C.; Vittori, S.; Mishra, R.C.; Dal Ben, D.; Klotz, K.N.; Volpini, R.; Cristalli, G. Synthesis and Biological Activity of Trisubstituted Adenines as A2A Adenosine Receptor Antagonists. *Nucleosides Nucleotides Nucleic Acids* **2007**, *26*, 1443–1446. [[CrossRef](#)]
20. Martire, A.; Lambertucci, C.; Peponi, R.; Ferrante, A.; Benati, N.; Buccioni, M.; Dal Ben, D.; Marucci, G.; Klotz, K.N.; Volpini, R.; et al. Neuroprotective potential of adenosine A1 receptor partial agonists in experimental models of cerebral ischemia. *J. Neurochem.* **2019**, *149*, 11–230. [[CrossRef](#)]
21. Takahashi, H.K.; Iwagaki, H.; Hamano, R.; Wake, H.; Kanke, T.; Liu, K.; Yoshino, T.; Tanaka, N.; Nishibori, M. Effects of adenosine on adhesion molecule expression and cytokine production in human PBMC depend on the receptor subtype activated. *Br. J. Pharmacol.* **2007**, *150*, 816–822. [[CrossRef](#)] [[PubMed](#)]
22. Wiwin, I.E.; Tatsuya, N.; Kazuyuki, K.; Yoshihiro, N. Focusing on Adenosine Receptors as a Potential Targeted Therapy in Human Diseases. *Cells* **2020**, *9*, 785.
23. Ohta, A.; Sitkovsky, M. Role of G-protein-coupled adenosine receptors in downregulation of inflammation and protection from tissue damage. *Nature* **2001**, *414*, 916–920. [[CrossRef](#)] [[PubMed](#)]
24. Minghetti, L.; Greco, A.; Potenza, R.L.; Pezzola, A.; Blum, D.; Bantubungi, K.; Popoli, P. Effects of the adenosine A2A receptor antagonist SCH 58261 on cyclooxygenase-2 expression, glial activation, and brain-derived neurotrophic factor availability in a rat model of striatal neurodegeneration. *J. Neuropathol. Exp. Neurol.* **2007**, *66*, 363–371. [[CrossRef](#)] [[PubMed](#)]
25. Orr, A.G.; Orr, A.L.; Li, X.J.; Gross, R.E.; Traynelis, S.F. Adenosine A2A receptor mediates microglial process retraction. *Nat. Neurosci.* **2009**, *12*, 872–878. [[CrossRef](#)]
26. Colella, M.; Zinni, M.; Pansiot, J.; Cassanello, M.; Mairesse, J.; Ramenghi, L.; Baud, O. Modulation of Microglial Activation by Adenosine A2A Receptor in Animal Models of Perinatal Brain Injury. *Front. Neurol.* **2018**, *9*, 605. [[CrossRef](#)]
27. Lasley, R.D.; Kristo, G.; Keith, B.J.; Mentzer, R.M. The A2a/A2b receptor antagonist ZM-241385 blocks the cardioprotective effect of adenosine agonist pretreatment in in vivo rat myocardium. *Am. J. Physiol. Heart Circ. Physiol.* **2007**, *292*, 426–431. [[CrossRef](#)]
28. Borea, P.A.; Gessi, S.; Merighi, S.; Vincenzi, F.; Varani, K. Pathological overproduction: The bad side of adenosine. *Br. J. Pharmacol.* **2017**, *174*, 1945–1960. [[CrossRef](#)]
29. Ongini, E.; Dionisotti, S.; Gessi, S.; Irenius, E.; Fredholm, B.B. Comparison of CGS 15943, ZM 241385 and SCH 58261 as antagonists at human adenosine receptors. *Naunyn-Schmiedeberg's Arch. Pharmacol.* **1999**, *359*, 7–10. [[CrossRef](#)] [[PubMed](#)]
30. Cristalli, G.; Palle, V.; Zablocki, J. Partial and Full Agonists of A1 Adenosine Receptors. 2004. Available online: <https://patentscope2.wipo.int/search/en/detail.jsf?docId=WO2004016635> (accessed on 22 February 2021).
31. Klotz, K.N.; Kachler, S.; Lambertucci, C.; Vittori, S.; Volpini, R.; Cristalli, G. 9-Ethyladenine derivatives as adenosine receptor antagonists: 2- and 8-substitution results in distinct selectivities. *Naunyn-Schmiedeberg's Arch. Pharmacol.* **2003**, *367*, 629–634. [[CrossRef](#)]
32. Salter, M.W.; Stevens, B. Microglia emerge as central players in brain disease. *Nat. Med.* **2017**, *23*, 1018–1027. [[CrossRef](#)] [[PubMed](#)]
33. Sachdeva, S.; Gupta, M. Adenosine and its receptors as therapeutic targets: An overview. *Saudi Pharm. J.* **2013**, *21*, 245–253. [[CrossRef](#)] [[PubMed](#)]
34. Franco, R.; Martínez-Pinilla, E.; Navarro, G.; Zamarbide, M. Potential of GPCRs to modulate MAPK and mTOR pathways in Alzheimer's disease. *Prog. Neurobiol.* **2017**, *149–150*, 21–38. [[CrossRef](#)]
35. Cunha, R.A. Neuroprotection by adenosine in the brain: From A(1) receptor activation to A(2A) receptor blockade. *Purinergic Signal.* **2005**, *1*, 111–134. [[CrossRef](#)] [[PubMed](#)]
36. Shakya, A.K.; Naik, R.R.; Almasri, I.M.; Kaur, A. Role and Function of Adenosine and its Receptors in Inflammation, Neuroinflammation, IBS, Autoimmune Inflammatory Disorders, Rheumatoid Arthritis and Psoriasis. *Curr. Pharm. Des.* **2019**, *25*, 2875–2891. [[CrossRef](#)] [[PubMed](#)]
37. Gomesa, C.V.; Kastera, M.P.; Tomé, A.R.; Agostinho, P.M.; Cunha, R.A. Adenosine receptors and brain diseases: Neuroprotection and neurodegeneration. *Biochim. Biophys. Acta* **2011**, *1808*, 1380–1399. [[CrossRef](#)] [[PubMed](#)]
38. Haskó, G.; Pacher, P.; Vizi, E.S.; Illes, P. Adenosine receptor signaling in the brain immune system. *Trends Pharmacol. Sci.* **2005**, *26*, 511–516. [[CrossRef](#)]
39. Sheth, S.; Brito, R.; Mukherjea, D.; Rybak, L.P.; Ramkumar, V. Adenosine Receptors: Expression, Function and Regulation. *Int. J. Mol. Sci.* **2014**, *15*, 2024–2052. [[CrossRef](#)]

40. Tsutsui, S.; Schnermann, J.; Noorbakhsh, F.; Henry, S.; Yong, V.W.; Winston, B.W.; Warren, K.; Power, C. A1 adenosine receptor upregulation and activation attenuates neuroinflammation and demyelination in a model of multiple sclerosis. *J. Neurosci.* **2004**, *11*, 1521–1529. [[CrossRef](#)] [[PubMed](#)]
41. Saura, J.; Angulo, E.; Ejarque, A.; Casadó, V.; Tusell, J.M.; Moratalla, R.; Chen, J.F.; Schwarzschild, M.A.; Lluís, C.; Franco, R.; et al. Adenosine A2A receptor stimulation potentiates nitric oxide release by activated microglia. *J. Neurochem.* **2005**, *95*, 919–929. [[CrossRef](#)]
42. Benveniste, E.N.; Benos, D.J. TNF-alpha- and IFN-gamma-mediated signal transduction pathways: Effects on glial cell gene expression and function. *FASEB J.* **1995**, *9*, 1577–1584. [[CrossRef](#)]
43. Zhu, B.T. Mechanistic explanation for the unique pharmacologic properties of receptor partial agonists. *Biomed. Pharmacother.* **2005**, *59*, 76–89. [[CrossRef](#)]
44. Clark, R.B.; Knoll, B.J.; Barber, R. Show all authors Partial agonists and G protein-coupled receptor desensitization. *Review* **1999**, *20*, 279–286.
45. Smalley, K.S.M.; Haass, N.K.; Brafford, P.A.; Lioni, M.; Flaherty, K.T.; Herlyn, M. Multiple signaling pathways must be targeted to overcome drug resistance in cell lines derived from melanoma metastases. *Mol. Cancer Ther.* **2006**, *5*, 1136–1144. [[CrossRef](#)] [[PubMed](#)]
46. Kitano, H. A robustness-based approach to systems-oriented drug design. *Nat. Rev. Drug Discov.* **2007**, *6*, 202–210. [[CrossRef](#)] [[PubMed](#)]
47. Zimmermann, G.R.; Lehar, J.; Keith, C.T. Multi-target therapeutics: When the whole is greater than the sum of the parts. *Drug Discov. Today* **2007**, *12*, 34–42. [[CrossRef](#)] [[PubMed](#)]
48. Podolsky, S.H.; Greene, J.A. Combination drugs—hype, harm, and hope. *N. Engl. J. Med.* **2011**, *365*, 488–491. [[CrossRef](#)]
49. Ghavami, S.; Shojaei, S.; Yeganeh, B.; Ande, S.R.; Jangamreddy, J.R.; Mehrpour, M.; Christoffersson, J.; Chaabane, W.; Moghadam, A.R.; Kashani, H.H.; et al. Autophagy and apoptosis dysfunction in neurodegenerative disorders. *Prog. Neurobiol.* **2014**, *112*, 24–49. [[CrossRef](#)]
50. Lopes, L.V.; Sebastião, A.M.; Ribeiro, J.A. Adenosine and related drugs in brain diseases: Present and future in clinical trials. *Curr. Top. Med. Chem.* **2011**, *11*, 1087–1101. [[CrossRef](#)]
51. Jacobson, K.A.; Tosh, D.K.; Jain, S.; Gao, Z.G. Historical and Current Adenosine Receptor Agonists in Preclinical and Clinical Development Front. *Cell. Neurosci.* **2019**, *13*, 124. [[CrossRef](#)]
52. Horita, T.K.; Kobayashi, M.; Mori, A.; Jenner, P.; Kanda, T. Effects of the adenosine A2A antagonist istradefylline on cognitive performance in rats with a 6-OHDA lesion in prefrontal cortex. *Psychopharmacology* **2013**, *230*, 345–352. [[CrossRef](#)]
53. Kondo, T.; Mizuno, Y.; Japanese Istradefylline Study Group. A long-term study of istradefylline safety and efficacy in patients with Parkinson disease. *Clin. Neuropharmacol.* **2015**, *38*, 41–46. [[CrossRef](#)]
54. Pinna, A. Adenosine A2A receptor antagonists in Parkinson's disease: Progress in clinical trials from the newly approved istradefylline to drugs in early development and those already discontinued. *CNS Drugs* **2014**, *28*, 455–474. [[CrossRef](#)] [[PubMed](#)]
55. Uchida, S.I.; Tashiro, T.; Kawai-Uchida, M.; Mori, A.; Jenner, P.; Kanda, T. The Adenosine A2A-Receptor. Antagonist Istradefylline Enhances the Motor Response of L-DOPA without Worsening Dyskinesia inMPTP-Treated Common Marmosets. *J. Pharmacol. Sci.* **2014**, *124*, 480–485. [[CrossRef](#)] [[PubMed](#)]
56. Agostini, M.; Tucci, P.; Melino, G. Cell death pathology: Perspective for human diseases. *Biochem. Biophys. Res. Commun.* **2011**, *28*, 414–451. [[CrossRef](#)] [[PubMed](#)]
57. Pietkiewicz, S.; SchmidtInna, J.H.; Lavrik, N. Quantification of apoptosis and necroptosis at the single cell level by a combination of Imaging Flow Cytometry with classical Annexin V/propidium iodide staining. *J. Immunol. Methods* **2015**, *423*, 99–103. [[CrossRef](#)] [[PubMed](#)]
58. Martí Navia, A.; Dal Ben, D.; Lambertucci, C.; Spinaci, A.; Volpini, R.; Marques-Morgado, I.; Coelho, J.E.; Lopes, L.V.; Marucci, G.; Buccioni, M. Adenosine Receptors as Neuroinflammation Modulators: Role of A<sub>1</sub> Agonists and A<sub>2A</sub> Antagonists. *Cells* **2020**, *9*, 1739. [[CrossRef](#)] [[PubMed](#)]
59. Antognoni, F.; Lianza, M.; Poli, F.; Buccioni, M.; Sntinelli, C.; Caprioli, G.; Iannarelli, R.; Lupidi, G.; Damiani, E.; Beghelli, D.; et al. Polar extracts from the berry-like fruits of *Hypericum androsaemum* L. as a promising ingredient in skin care formulations. *J. Ethnopharmacol.* **2017**, *195*, 255–265. [[CrossRef](#)]
60. Fezai, M.; Slaymi, C.; Ben-Attia, M.; Kroemer, G.; Lang, F.; Jemaa, M. Inhibition of Colon Carcinoma Cell Migration Following Treatment with Purified Venom from Lesser Weever Fish (*Trachinus Viper*). *Cell. Physiol. Biochem.* **2017**, *41*, 2279–2288. [[CrossRef](#)] [[PubMed](#)]
61. Viswanathan, A.; Zhurina, A.; Assoah, B.; Paakkunainen, A.; Musa, A.; Kute, D.; Saravanan, K.M.; Yli-Harja, O.; Candeias, N.R.; Kandhavelu, M. Decane-1,2-diol derivatives as potential antitumor agents for the treatment of Glioblastoma. *Eur. J. Pharmacol.* **2018**, *837*, 105–116. [[CrossRef](#)]